Anal. Chem. **2001,** *73,* 151−156

Articles

Full Phase Analysis of Portland Clinker by Penetrating Synchrotron Powder Diffraction

Ángeles G. de la Torre,[†] Aurelio Cabeza,[†] Ana Calvente,[‡] Sebastián Bruque,[†] and Miguel A. G. Aranda*,[†]

Departamento de Química Inorgánica, Cristalografía y Mineralogía, Universidad de Málaga, 29071 Málaga, Spain, and Italcementi Group, Cementos Goliat, Ctra. Málaga-Almería km 8, 29720 Málaga, Spain

Fabrication of portland cements commonly depends on X-ray fluorescence (XRF), which measures the elemental compositions. XRF is used to adjust the raw material proportions and to control the process conditions. However, to predict the mechanical strength of the resulting concrete, it is essential to know the phase composition which is, so far, indirectly inferred by the Bogue method. Here, we report a phase analysis of an industrial portland clinker containing six crystalline phases, Ca_3SiO_5, Ca_2SiO_4, $Ca_4Al_2Fe_2O_{10}$, $Ca_3Al_2O_6$, $NaK_3(SO_4)_2$, and CaO, by Rietveld refinement of synchrotron X-ray powder diffraction data ($\lambda = 0.442\ 377$ Å). Even the minor component, CaO 0.45(2)%, was readily analyzed. We have also carried out a phase study of the same clinker with laboratory X-rays to characterize the changes in the detection limit and errors. Furthermore, by adding a suitable crystalline standard to the same clinker, we have determined the overall amorphous phase content. The procedure established for this state-of-the-art phase analysis shows the high precision that can be achieved by using penetrating X-rays, which is of interest not only in cement chemistry but in other industrially important multiphase systems such as slags, superalloys, or catalysts.

Portland clinkers and cements are complex materials of world importance, and the mineralogical quantification of portland cement is necessary to predict the performances of the resulting concrete. The hydraulic properties of a concrete depend on the cement mineralogical composition and on its texture. The Bogue method[1] estimates the four main phase fractions (alite, Ca_3SiO_5,C3S; belite, Ca_2SiO_4, C2S; ferrite, $Ca_4Al_2Fe_2O_{10}$, C4AF; aluminate, $Ca_3Al_2O_6$, C3A) of clinker from the elemental composition, usually determined by X-ray fluorescence (XRF), by assuming thermal equilibrium at high temperature. This method bears a wide error margin as it relies on various conditions that usually are not held. To partly compensate that, mechanical assays of set cements are carried out a fortiori, by which time the performance of the cements cannot be modified.

On the other hand, laboratory X-ray powder diffraction (LXRPD) it is now routinely used for measuring crystalline phase ratios of simple systems[2,3] by using the Rietveld method.[4] No internal standard is needed, but the crystal structures must be known as the process consists of the comparison between the measured and the calculated patterns. The application to clinkers is not straightforward for the following reasons: (a) there are many phases, usually more than five, each with its own mass absorption coefficient; (b) the small mean penetration depth of X-rays (∼30 μm for Cu Kα) implies that a thin layer only is analyzed in the Bragg−Brentano $\theta/2\theta$ geometry leading to poor particle statistics; (c) some phases, for instance, alite, crystallize as plaquets which show preferred orientation effects; (d) phases can crystallize as several polymorphs[5] that must be identified a priori; (e) there is strong peak overlapping; (f) the diffraction peak broadening is usually anisotropic; and (g) the atomic impurities inside each phase are not known. LXRPD has been extensively used in cement studies;[6,7] however, a round-robin study on the accuracy and precision of cement phase quantification studied by three techniques, including quantitative LXRPD, did not yield satisfactory results.[8] Quantification of a mixture of synthetic C3S and C2S silicates has been reported by Rietveld refinement[9] and similar studies for industrial portland cement are actually being carried out[10,11] although subject to considerable errors if the analysis procedure is not properly tested. Full phase quantification of clinkers and cements using powder diffraction has been a challenge for a century.

Penetrating synchrotron X-ray powder diffraction (SXRPD) overcomes most of these drawbacks. As the X-rays are highly energetic, the absorption is minimized, which helps points a and

* To whom the correspondence should be addressed: g_aranda@uma.es.
[†] Universidad de Málaga.
[‡] Cementos Goliat.

(1) Bogue, R. H. *Ind. Eng. Chem., Anal. Ed.* **1929**, *1*, 192.
(2) Hill, R. J.; Howard, C. J. *J. Appl. Crystallogr.* **1987**, *20*, 467.
(3) Bish, D. L.; Howard, S. A. *J. Appl. Crystallogr.* **1988**, *21*, 86.
(4) Rietveld, H. M. *J. Appl. Crystallogr.* **1969**, *2*, 65.
(5) Taylor, H. F. W. *Cement Chemistry*; Thomas Telford: London, 1997; p 1−28.
(6) Glasser, F. P. In *Lea's Chemistry of Cement and Concrete*; Hewlett, P. C., Ed.; Arnold: London, 1998; pp 196−227.
(7) Gutteridge, W. A. *Br. Ceram. Proc.* **1984**, *35*, 11.
(8) (a) Aldrige, L. P. *Cem. Concr. Res.* **1982**, *12*, 381; (b) Aldrige, L. P. *Cem. Concr. Res.* **1982**, *12*, 437.
(9) Neubauer, J.; Sieber, R. *Mater. Sci. Forum* **1996**, *228−231*, 807.
(10) (a) Neubauer, J. *Proceedings of the 20th International Conference on Cement Microscopy*, Guadalajara, Mexico, 1998, p 103−119; (b) Feret, B.; Feret, C. F. *Cem. Concr. Res.* **1999**, *29*, 1627.
(11) Taylor, J. C.; Hinczak, I.; Matulis, C. E. *Powder Diffr.* **2000**, *15*, 7.

10.1021/ac0006674 CCC: $20.00
Published on Web 12/15/2000

Table 1. Elemental[a] and Phase Compositions for the Portland Clinker from XRF Analysis,[b] and SXRPD and $L_{(1)}$XRPD Rietveld Refinements

elements / phases	XRF (%)	SXRPD (%)	LXRPD (%)	L_1XRPD (%)
CaO	64.14	65.32		
SiO_2	21.20	22.30		
Al_2O_3	5.70	6.78		
Fe_2O_3	3.45	3.67		
Na_2O	0.18[c]	0.18		
K_2O	1.26[c]	0.82		
SO_3	1.72[d]	0.93		
C	1.9[e]	0.42(2)	*g*	*g*
C3S	48.96[f]	48.6(2)	52.3(5)	50.7(7)[h]
C2S	24.12[f]	27.3(2)	25.7(7)	25.8(9)[h]
C4AF	10.49[f]	15.6(5)	14.2(4)	15.7(5)[h]
C3A	9.27[f]	6.18(7)	5.6(2)	6.1(3)[h]
NKS		1.93(6)	2.2(3)	1.7(2)[h]

[a] Elemental analysis is expressed as parent oxide content. [b] MgO was 1.38%. [c] Na and K determined from emission spectroscopy. [d] SO_3 determined from gravimetry. [e] CaO determined from titrimetry. [f] Obtained by the Bogue method. [g] CaO not detected. [h] Values derived by normalizing the refined fractions using 21.2% Al_2O_3.

b above and is the *key* to a successful analysis. Working in transmission (rotating capillary geometry), the full sample is analyzed as in neutron diffraction and preferred orientation, point c, is not a problem. High-resolution data also help to minimize the problems stated in (d−f) although for strong broadening coming from crystallites size and strain effects, the improving in (f) may be marginal. To tackle point g is more problematic; if necessary, analytical electron microscopy can be used. In this work, we will show the possibilities of **q**uantitative SXRPD (QSXRPD) for characterizing very complex materials.

EXPERIMENTAL SECTION

The clinker used in this study was sampled from the Goliat rotary kiln (Málaga, Spain) operating under normal conditions on 11-Nov-98. The elemental composition was determined by XRF on a Philips PW 1660 spectrometer using the borate glass bead sample preparation method, which minimizes matrix effects. Na and K contents cannot be accurately determined by XRF because they are volatile. Hence, Na and K chemical analyses were carried out by atomic emission spectroscopy. The clinker was heated with lithium borate and then dissolved in hydrochloric acid. Overall free calcium oxide content was measured by titrimetry of the calcium glycerolate obtained by refluxing. The sulfate content was determined gravimetrically as $BaSO_4$. The measured elemental analysis and the estimated phase fractions, by the Bogue method, are given in Table 1.

The SXRPD pattern was collected on the BM16 diffractometer of ESRF in Debye−Scherrer (transmission) configuration. The clinker was loaded in a borosilicate glass capillary (diameter 1.0 mm), rotated during data collection and irradiated with a short wavelength, 0.442 377(2) Å (≡28.03 keV), selected with a double-crystal Si (111) monochromator. The run between 3 and 30° (2θ) lasted 2.5 h, and the data were normalized and summed up to 0.003° step size. The LXRPD pattern was recorded on a Siemens D5000 $\theta/2\theta$ diffractometer (flat reflection mode) by using Cu $K\alpha_{1,2}$ radiation, 1.542 Å (≡8.04 keV) with a secondary curved graphite monochromator. The clinker was loaded in an aluminum holder by gently sample-front pressing. The 2θ range was 10−70°, in 0.03° steps, counting by 25 s/step. The holder was not spun during data collection as our D5000 diffractometer does not have that attachment. A third pattern for the clinker mixed with Al_2O_3 was recorded between 10 and 70°, in 0.02° steps, counting by 25 s. To minimize overlapping, a Philips X′PERT $\theta/2\theta$ diffractometer with strictly monochromatic Cu $K\alpha_1$ radiation, 1.540 598 Å, [Ge (111) primary monochromator] was used, L_1XRPD data. Sample-front loading was also used.

RESULTS AND DISCUSSION

The powder patterns were analyzed by the Rietveld method[4] with the GSAS suite of programs[12] by using the pseudo-Voigt peak shape function[13] corrected for axial divergency.[14] First, we studied the SXRPD pattern. The main phase, C3S, has anisotropic line-shape broadening which was fitted by using a new approach based of multidimensional distribution of lattice metrics.[15] This is a new phenomenological approach to describe anisotropic broadening with few parameters, and it leads to optimal peak-shape fits. Some other minor phases also showed anisotropic line-shape broadening, which was corrected by using the less powerful "ellipsoidal broadening", but with less adjustable parameters, to not over-parametrize the refinements. The highly resolved SXRPD data with excellent signal-to-noise ratio allowed the selection of the best polymorph to describe a given phase as it must yield the lowest disagreement factors. To do so, the pattern was fitted with the possible crystal structures and we evaluated the phase-dependent, R_F, and pattern-dependent, R_{WP}, R factors.[4,12] The main phase, alite, has seven polymorphs[16] and the complex monoclinic superstructure[17] gave the best fit. The second phase, belite, has five polymorphs[18] and the monoclinic structure, β-phase,[19] gave a very good fit. The body-centered orthorhombic polymorph[20] yielded the best fit for ferrite. Aluminate may crystallize in four polymorphs,[21] and the cubic phase[22] was the most appropriated to describe this component. Free crystalline CaO, C, was observed but MgO was not detected. Finally, a few peaks were not accounted for. Several sulfates were checked and only one, aphthitalite $NaK_3(SO_4)_2$ NKS,[23] gave a good fit.

The calculated powder patterns of C3S and C2S using the reported structural parameters are displayed in Figure 1. For C2S, there is a wide agreement that β-polymorph[19] is the most adequate structure and we can confirm that. However, there is a recent report[11] claiming that the triclinic polymorph of C3S is present in clinkers. The calculated powder pattern of triclinic C3S (top of

(12) Larson, A. C.; Von Dreele, R. B. *Los Alamos National Lab. Rep. No. LA-UR-86-748*, Los Alamos, 1994. GSAS program @ http://public.lanl.gov: 80/gsas/.
(13) Thompson, P.; Cox, D. E.; Hasting, J. B. *J. Appl. Crystallogr.* **1987**, *20*, 79.
(14) (a) Finger, L. W.; Cox, D. E.; Jephcoat, A. P. *J. Appl. Crystallogr.* **1994**, *27*, 892. (b) Aranda, M. A. G.; Losilla, E. R.; Cabeza, A.; Bruque, S. *J. Appl. Crystallogr.* **1998**, *31*, 16.
(15) Stephens, P. W. *J. Appl. Crystallogr.* **1999**, *32*, 281.
(16) Taylor, J. C.; Aldrige, L. P. *Powder Diffr.* **1993**, *8*, 138.
(17) Nishi, F.; Takeuchi, Y.; Maki, I. *Zeit. Kristallogr.* **1985**, *172*, 297.
(18) Mumme, W.; Cranswick, L.; Chakoumakos, B. *Neues Jahrb. Miner. Abh.* **1996**, *170*, 171.
(19) Mumme, W. G.; Hill, R. J.; Bushnell-Wye, G.; Segnit, E. R. *Neues Jahrb. Miner. Abh.* **1995**, *169*, 35.
(20) Colville, A. A.; Geller, S. *Acta Crystallogr.* **1971**, *B27*, 2311.
(21) Goetz-Neunhoeffer, F.; Neubauer, J. *Proceedings of the 10th International Congress of Chemistry of Cements*, Göteborg, Germany, 1997; Vol. 1, p li056−64.
(22) Mondal, P.; Jeffery, J. W. *Acta Crystallogr.* **1975**, *B31*, 689.
(23) Okada, K.; Ossaka, J. *Acta Crystallogr.* **1980**, *B36*, 919.

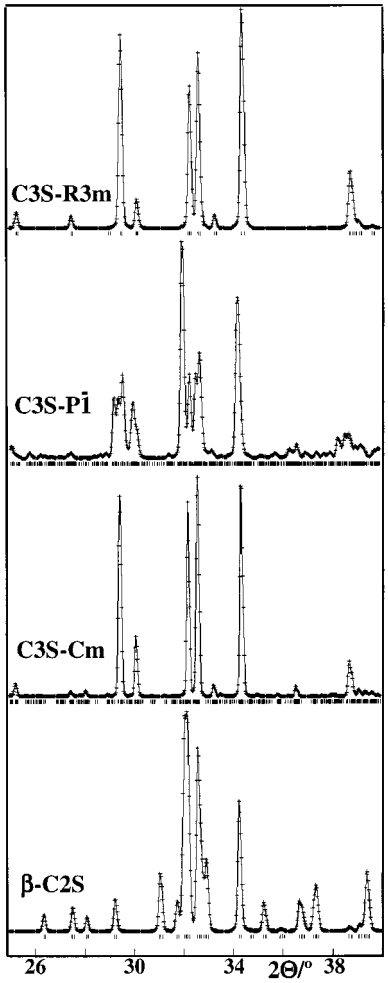

Figure 1. Calculated powder patterns for C3S (rhombohedral),[26] C3S (triclinic),[24] C3S (monoclinic-*Cm* superstructure),[17] and C2S (β polymorph)[19] for Cu K$\alpha_{1,2}$ radiation.

Figure 1 in ref 11) by Taylor et al. does not agree with our simulation (based on the same reported structure)[24] shown in Figure 1. Our calculated pattern fully agrees with the simulated pattern included in the powder diffraction file (PDF; file 70-1846) computed using a different program. So, the conclusions of that work[11] about the presence of triclinic C3S in clinkers should be taken very cautiously as they have had problems in the C3S powder pattern simulation. With very high resolution SXRPD data, we can conclusively rule out the presence of the triclinic polymorph of C3S in our industrial sample. In Figure 2 are shown the calculated powder patterns of C4AF, C3A, and NKS using the reported structures.

The positional parameters of the phases were not varied and an overall isotropic temperature factor, $U_{iso} = 0.01$ Å^2, was used. The Fe/Al ratios, constrained to full occupancies, were refined for C4AF. Fe content converged to 54(2)% at (0 0 0) and to 15-(1)% at (0.928 1/4 0.953). This result agrees with single phase refinements.[20,25] The last refinement for the SXRPD pattern converged to $R_{WP} = 7.54\%$ and $R_P = 5.41\%$. The refined weight

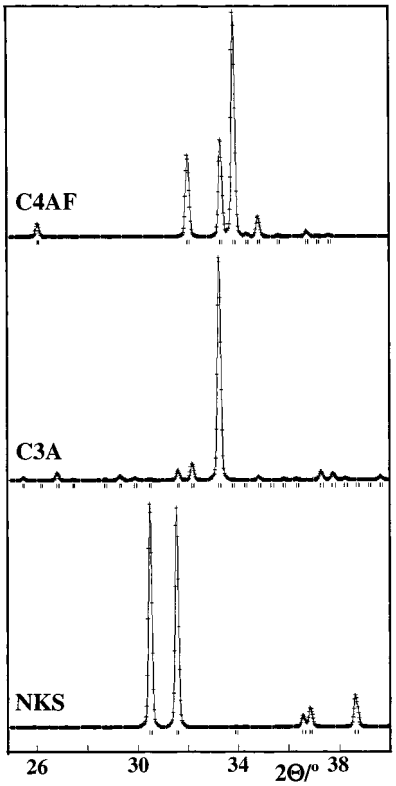

Figure 2. Calculated powder patterns for C4AF,[20] C3A,[22] and NKS[23] for Cu K$\alpha_{1,2}$ radiation.

fractions from this analysis and the derived elemental composition are given in Table 1. Details of the SXRPD Rietveld refinement are given in Table 2. The phases related with the crystallization of the liquid existing in the kiln, C4AF, C3A, and NKS, have much broader diffraction peaks; see Table 2. The Rietveld plot is displayed in Figure 3 and an enlarged view of the most informative region of this pattern is given in Figure 4.

In the refinements of the laboratory data, we used the polymorphs and anisotropic peak-broadening directions determined in the former SXRPD study. The overall parameters were varied and the phase scale factors were optimized. Diffraction peaks of crystalline CaO were not detected in the L_1XRPD studies. C3S crystallizes as pseudohexagonal multitwinned plaquets. So, its powder pattern can show preferred orientation. In the monoclinic setting, the hexagonal *c* axis direction becomes [−101]. So, we have applied the March−Dollase correction along this direction, which greatly improves the fits of laboratory data. We check this correction for the SXRPD data, and it did not improve the fit; the coefficient converged to 1.002(2). So, the pattern collected in a rotating capillary does not show preferred orientation, as expected. However, the flat samples in LXRPD and L_1XRPD studies did show this effect with refined parameters 0.922(6) and 0.895(5), respectively. The resolution in the L_1XRPD patterns is much lower than that in the SXRPD pattern. So, we used a anisotropic pseudo-Voigt function for the peaks of C3S by refining GW (the Gaussian part), LY (the Lorentzian part), and STEC (the anisotropic correction of the Lorentzian width) along [100] in the laboratory studies. The peaks of the remaining phases were fitted with a Lorentzian function with anisotropic broadening, if necessary, as determined in the SXRPD study. The phase

(24) Golovastikov, R.; Matveeva, R. G.; Belov, N. V. *Sov. Phys. Cryst.* **1975**, *20*, 441.
(25) Berliner, R.; Ball, C.; West, P. B. *Cem. Concr. Res.* **1997**, *27*, 551.
(26) Ilinets, A. M.; Malinovskii, Y.; Nevskii, N. N. *Dokl. Akad. Nauk SSSR* **1985**, *281*, 332.

Table 2. Selected Data for the SXRPD Rietveld Refinement of Portland Clinker[a]

phase	sg	a (Å)	b (Å)	c (Å)	β (deg)	V (Å^3)	GW (0.01°)^2	LY (0.01°)	STEC (0.01°)	R_F (%)
C3S	C m	33.0942(5)	7.0558(2)	18.5709(3)	94.232(1)	4324.6(1)	0.16(2)	b	b	2.84
C2S	$P\,2_1/n$	5.5145(2)	6.7645(2)	9.3367(3)	94.387(3)	347.26(2)	0.96(9)	30.4(9)	17(1)[c]	2.02
C4AF	$I\,bm2$	5.5326(3)	14.5720(6)	5.3290(3)	90.0	429.63(3)	0.4(1)	77(2)	−24(2)[d]	1.45
C3A	$P\,a\bar{3}$	15.2459(3)	15.2459	15.2459	90.0	3543.7(2)	0.5(1)	33(1)	−	2.50
NKS	$P\,\bar{3}m1$	5.6723(4)	5.6723	7.313(1)	90.0	203.79(4)	0.1(−)	46(3)	38(4)[e]	2.09
C	$F\,m\bar{3}m$	4.8058(1)	4.8058	4.8058	90.0	110.99(1)	0.1(−)	8.7(8)	−	1.29

[a] S/L = 0.0072 and H/L = 0.0039 values were used to describe the asymmetry due to axial divergence for all phases. [b] The anisotropic shape function[15] used to fit the diffraction peaks had the following parameters: eta = 0.55(1), $S_{400} = 1.71(7) \times 10^{-4}$, $S_{040} = 0.54(1)$, $S_{004} = 5.6(2) \times 10^{-3}$, $S_{220} = S_{202} = 0$, $S_{022} = 3.9(2) \times 10^{-2}$, $S_{310} = 3.9(2) \times 10^{-4}$, $S_{103} = -2.47(6) \times 10^{-3}$, and $S_{031} = -1.25(8) \times 10^{-2}$. [c] Anisotropic peak-broadening directions for ellipsoidal correction: [0 0 1]. [d] Anisotropic peak-broadening directions for ellipsoidal correction: [1 2 0]. [e] Anisotropic peak-broadening directions for ellipsoidal correction: [0 0 1].

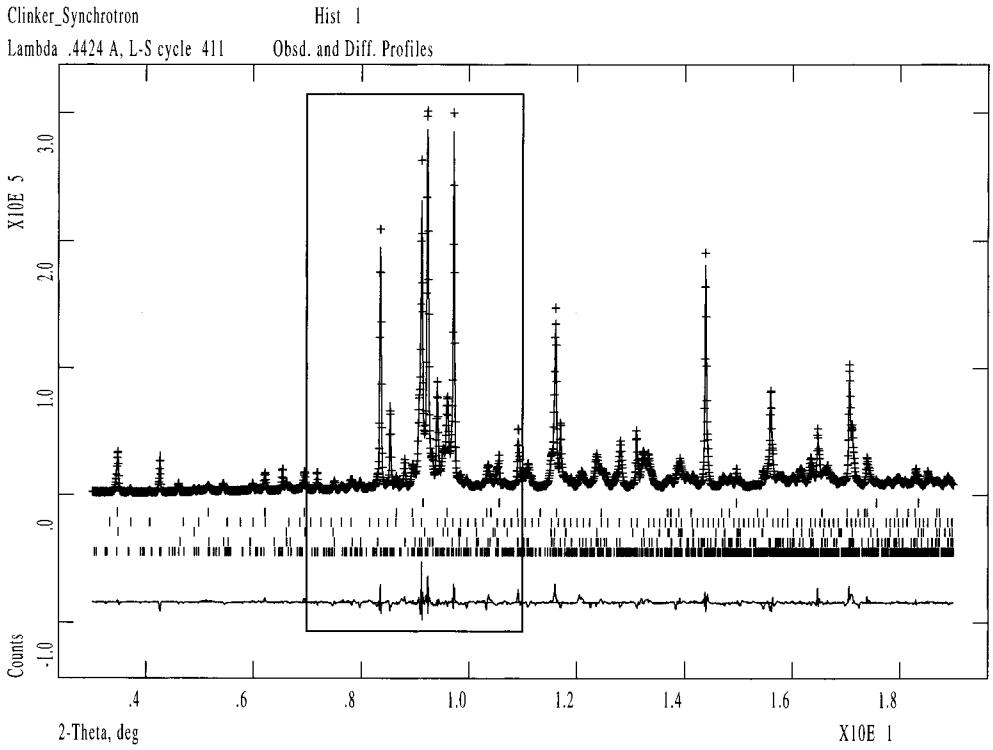

Figure 3. SXRPD Rietveld plot (3−19°/2θ) for the portland clinker with the observed (crosses), calculated (line), and difference (bottom line) powder patterns. The marks correspond to the Bragg peaks of the different phases; from bottom to top: C3S, C2S, C4AF, C3A, NKS, and C.

fractions determined in the L_1XRPD analyses are also given in Table 1.

By adding a suitable standard with negligible amorphous phase content, the Rietveld method can determine the overall amorphous phase ratio in the sample. To do so, a weighted amount of standard is thoroughly ground with the sample. The crystalline phases present in the sample have smaller refined weight ratios than those calculated from the weight mixture because of the presence of the amorphous phase(s). So, from the overestimation of the standard, the overall amorphous phase content is deduced. The amorphous content, A, is obtained from the following equation: $\% A = (1 - W_S/R_S)(100 - W_S)^{-1} \times 10^4$, which can be easily derived, and where W_S stands for the weighted concentration of the internal standard and R_S stands for the Rietveld analyzed concentration of the internal standard.

In this particular case, we used Al_2O_3, which has a negligible amorphous fraction because it was heated at 1350 °C for 4 h. Furthermore, this compound has a mass absorption coefficient similar to those of the main phases of the clinker. We used strictly monochromatic X-rays to reduce the overlapping of the diffraction peaks. 20.00% (W_S) in weight of Al_2O_3 was added to the clinker and the Rietveld refinement converged to 21.17(27)% (R_S). So, the these values indicate 6.9(1.6)% of amorphous phase(s) in the clinker. The R factors were $R_{WP} = 10.8$ and 10.9% for LXRPD and L_1XRPD, respectively. The Rietveld plots are given in Figures 5 and 6.

Although the amorphous content is not negligible, the low ratio allows the reliable comparison between the XRF study, overall sample, and the SXRPD study, crystalline part, Table 1. Some approximations were applied in the Rietveld analyses; i.e., the Mg content in Ca_3SiO_5 could not be determined as the superstructure is very complex ($V \sim 4325$ Å^3). So, Ca content from SXRPD is slightly overestimated, Table 1. The superstructure description of C3S[17] is only approximate and may be slightly sample dependent, which makes its fit a bit problematic. Free CaO determined by titrimetry includes CaO and amorphous basic species. So,

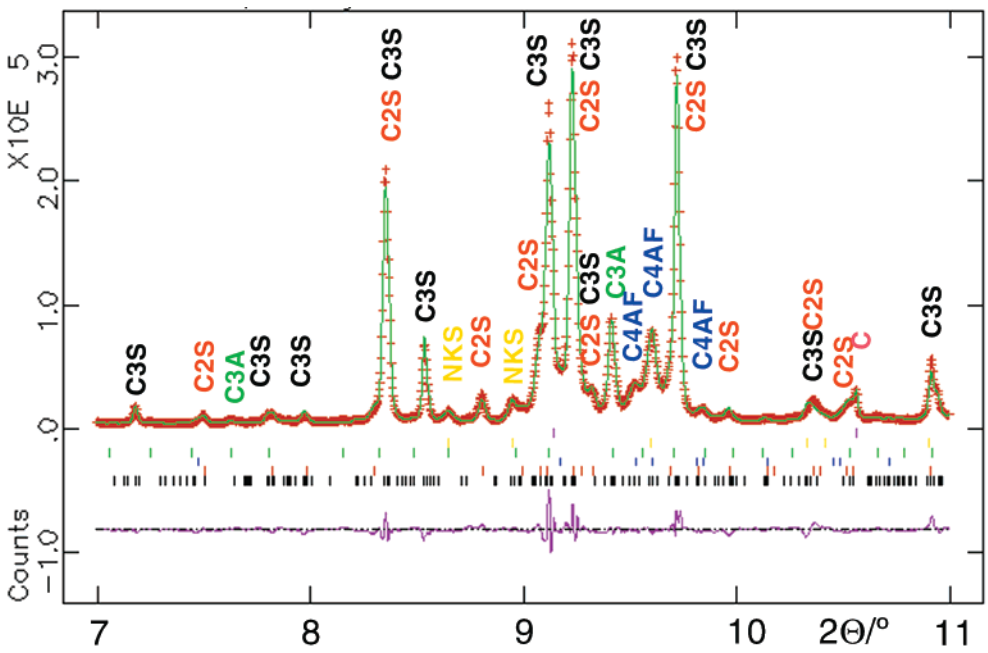

Figure 4. Representative region of the SXRPD Rietveld plot for portland clinker with the observed (red crosses), calculated (green line), and difference (pink line) powder patterns. The colored ticks show the allowed Bragg reflections for C3S (black), C2S (red), C4AF (blue), C3A (green), NKS (yellow), and C (pink). The peaks mainly due to a given phase are labeled.

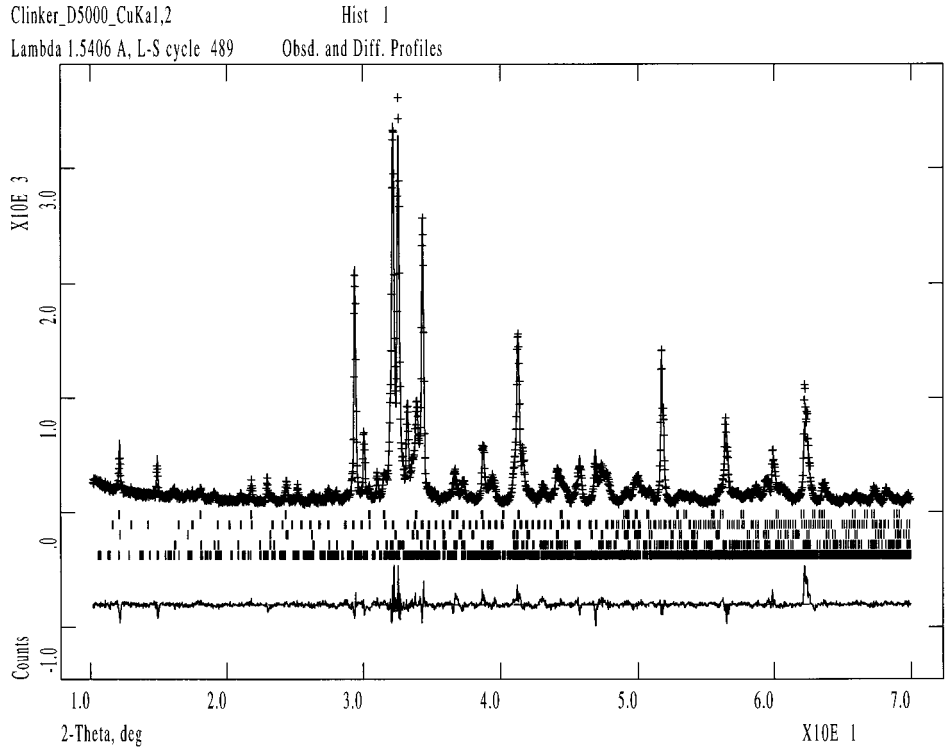

Figure 5. LXRPD Rietveld plot (10−70°/2θ) for the portland clinker as in Figure 3.

crystalline unreacted CaO content from SXRPD must be smaller, as observed. The presence of amorphous phase is in agreement with the observation that K and S contents are underestimated in the Rietveld refinement, and the chemical analysis (overall sample) clearly indicates a higher alkaline sulfate content. Taking into account these approximations, there is a satisfactory agreement between the measured elemental composition and that derived from the SXRPD study, Table 1. Hence, the reported procedure yields a precise and accurate phase analysis.

The results from L_1XRPD are obviously not as good as those obtained from SXRPD. The main problem arise from the strong overlapping between the peaks of C3S and C2S. The laboratory refinements slightly overestimate the C3S content and underestimate the C2S content; see Table 1. CaO is present in the SXRPD pattern, but it could not be detected in the LXRPD and L_1XRPD studies. This is likely due to the hydration of lime to yield amorphous portlandite. It must be noted that LXRPD and L_1XRPD patterns were collected one month after the SXRPD study.

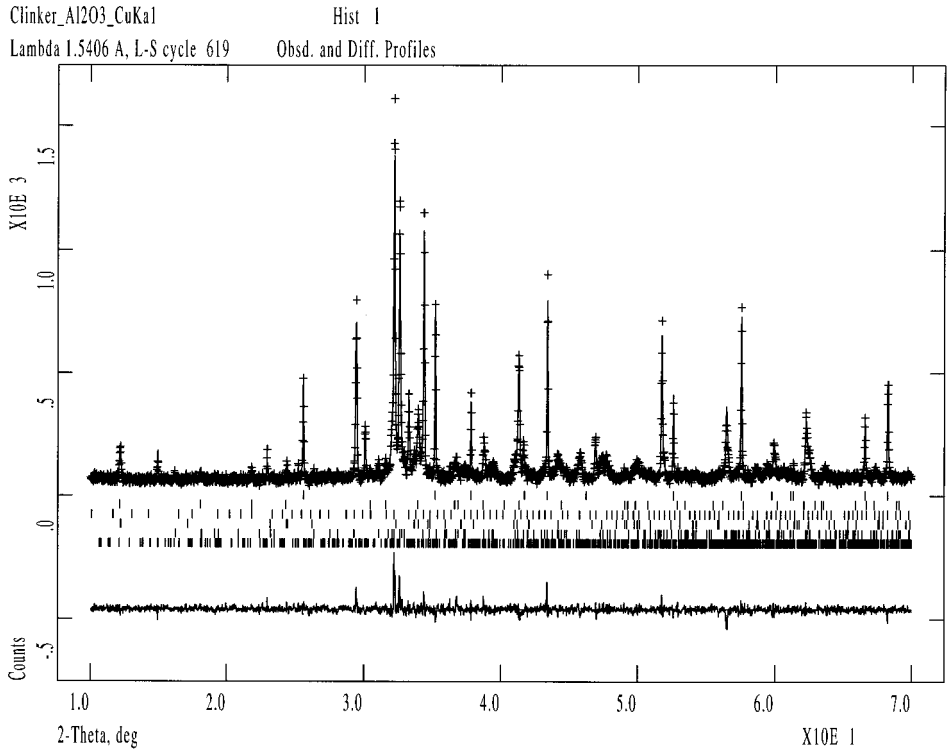

Figure 6. L_1XRPD Rietveld plot (10−70°/2θ) for the portland clinker mixed with Al_2O_3 (top phase) as in Figure 3.

Although the sample was kept in a dry atmosphere, hydration could take place during sample manipulation and data collection. To check that, we have carried out a thermal analysis study (TGA and DTA) of the clinker 23 months after its prepartion and 19 months after SXRPD data collection. These data have been collected on a Rigaku Thermoflex apparatus at the heating rate 10 K min^{-1} in air with calcined Al_2O_3 as internal reference standard. Two endotherms centered at 455 and 685 °C were observed. The weight losses associated to these endotherms were 0.15 and 0.75%, respectively. The first endothermic effect is due to the water loss of portlandite, and the second one is due to the decomposition of $CaCO_3$ formed by the carbonation of portlandite. From these weight losses, it is possible to determine the pristine CaO content that produced $Ca(OH)_2$ and $CaCO_3$ with time. A total of 0.47% CaO reacted to give portlandite, and 0.96% of CaO is hydrated and later carbonated to yield amorphous calcite. Hence, the CaO content determined by TGA−DTA data is 1.43%, which is slightly lower than the overall content, 1.9%, determined by titrimetry.

The presence of Cu $K\alpha_{1,2}$ doublets raises errors that are harmful for low concentration phases, Table 1. Furthermore, minor phases with large peak broadening are difficult to quantify as the description of the broadening correlates slightly with the phase scale factors. The results from L_1XRPD are better than those from LXRPD although a seventh phase was added. This clearly shows that the best possible resolution is essential to obtain a good phase analysis of a complex material. To establish correlations between major phases (C3S and C2S) and some physical and mechanical properties LXRPD data can be used. If possible, strictly monochromatic laboratory X-rays should be used. For initial calibrations and to obtain accurate results, high-energy SXRPD data are very recommendable.

It must be noted that an on-line XRD instrument capable of continuous analysis of either cement or clinker stream has been very recently reported.[27] A prototype has been installed in a cement plant giving very good results. Finally, we would like to speculate on the *future* use of LXRPD to follow on-line fabrication of industrially important complex materials. A new goniometer-free setup will probably be implemented with a high-energy X-ray tube, i.e., Ag Kα (0.559 Å ≡ 22.2 keV), as radiation source and a charge-coupled detector (CCD) as a bidimensional detector. The system will work in transmission with the sample in a capillary. The detector pixel size and the sample-to-detector distance will define the resolution. Data will be collected in seconds and the automated Rietveld analysis of a selected region, obtained by calibrated integration of the Debye-rings, will allow determination of the phase composition within minutes. This system combines the advantages of penetrating X-rays, already demonstrated in this work, and the fast 2D detection system, which avoids sample-related effects such as texture. The ultimate goal is to carry out the type of analysis reported here but in-house, routinely, faster, and inexpensively.

ACKNOWLEDGMENT

We thank Dr. Olivier Masson for assistance during SXRPD data collection and to ESRF for the provision of synchrotron facilities. L_1XRPD data were recorded in ICMM (CSIC, Madrid) which is thanked. This work has been supported by the FEDER 1FD97-0894 research grant.

Received for review June 12, 2000. Accepted October 31, 2000.

AC0006674

(27) Manias, C.; Retallack, D.; Madsen, I. *World Cem.* **2000**, (Feb). 78.